2008 American Control Conference
Westin Seattle Hotel, Seattle, Washington, USA
June 11-13, 2008



# Adaptive control of time-varying systems with gain-scheduling

Jinho Jang, Anuradha M. Annaswamy, and Eugene Lavretsky

*Abstract*— **In this paper, we address the problem of controlling a nonlinear system in the presence of parametric uncertainties. The adaptive controller proposed includes a a nominal controller which is based on gain-scheduling and an adaptive component where adjustable parameters are self-tuned in order to accommodate the system uncertainties. The resulting closed-loop system is shown to have globally bounded solutions when the command signals that need to be tracked vary sufficiently slowly. The reported stability results are validated using nonlinear flight simulation models of a high performance aircraft.**

## I. INTRODUCTION

One of the popular methods of nonlinear control design is the gain-scheduling [1], [2] and it has been used in a wide range of applications including flight control [3], [4], process control [5], and wind-turbine control [6]. The main idea behind the gain-scheduling approach is to decompose the nonlinear control design task into a family of linear control design methods and schedule this family of linear controllers based on the command signal so as to ensure that the original nonlinear system follows the desired dynamics. When the gain-scheduled variable is slowly varying, stability results of almost time-invariant systems can be called upon to establish stability of the underlying closed-loop linear time-varying system and therefore to assess stability properties of the original nonlinear system [1], [2].

Often, the nonlinear control problem discussed above is faced with yet another difficulty, which is the presence of uncertainties due to modeling errors, unknown aerodynamics, as well as anomalies in the control inputs. Actuators are often affected by a number of factors including control saturation, degradation of control effectiveness, or control failures. It is therefore important that a gain-scheduled controller designed using the procedures described in [1], [2] is able to adequately cope with any or all of the uncertainties mentioned above. This motivates the problem considered in this paper. It is shown that by augmenting a gain-scheduling controller with an adaptive controller, the desired behavior of the original nonlinear closed-loop dynamics can be achieved, if the gain-scheduled variable changes sufficiently slowly. In [7], adaptive gain-scheduling controllers are proposed for HVDC systems, where in simulations it is shown that they result in a better performance. In this paper, a formal description to construct an adaptive gain-scheduled controller is provided as well as stability analysis for nonlinear flight dynamics.

This work was supported by the Boeing Strategic University Initiative.

Jinho Jang is with the Department of Mechanical Engineering, MIT, Cambridge, MA 02139, USA. jinho@mit.edu

Anuradha M. Annaswamy is with the Department of Mechanical Engineering, MIT, Cambridge, MA 02139, USA. aanna@mit.edu

Eugene Lavretskyis is with the Boeing Company, Huntington Beach, CA 92647, USA. eugene.lavretsky@boeing.com

## II. PROBLEM STATEMENT

We consider a nonlinear plant of the form

$$\dot{X} = F(X) + G(X)U. \tag{1}$$

where $X \in \Re^n$ is the system state and $U \in \Re^m$ represents the control input. It is assumed that the system can be written as

$$\begin{aligned} \dot{X}_p &= f(X_p, X_g) + g(X_p, X_g)U_1 \\ \dot{X}_g &= h(X_g, U_2) \end{aligned} \tag{2}$$

where the system state $X$ is partitioned into two vector components, $X_p \in \Re^{n_p}$ and $X_g \in \Re^{n_g}$, so that the former represents the fast changing controlled output, relative to the slow state component $X_g$. The latter will become the gain-scheduled variable. It is also assumed that sufficient information is available about the nonlinearity $h$ so that an outer-loop controller, $U_2 = h_c(X_g, X_{g_c})$, can be chosen so that $X_g(t)$ tracks $X_{g_c}(t)$, its desired command signal, and satisfies the following assumption:

**Assumption 1.** *$X_{g_c}(t)$ is continuously differentiable and slowly varying, i.e.*

$$\left\|\dot{X}_{g_c}(t)\right\| < \varepsilon_1, \quad \forall t \geq t_0. \tag{3}$$

The problem is to design $U_1$ in (2) such that the controller ensures that the closed-loop system has globally bounded solutions in the presence of parametric uncertainties in $f$ and $g$. In order to control the nonlinear system in (2) for arbitrary initial conditions and a large family of command signals, we consider a family of operating points in the vicinity of $X_{g_c}(t)$ as

$$\sigma_g = \left\{X_{g,1},\ X_{g,2},\ \cdots,\ X_{g,k}\right\}. \tag{4}$$

The dimension of $X_{g,i}$ is $n_g$ and its $r$th component is $X_{g_r,i}$.

**Definition 1.** *$X_{g,i}$ and $X_{g,j}$ are separated operating points if $X_{g_r,i} \neq X_{g_r,j}$ for $1 \leq i,\ j \leq k$ and $1 \leq r \leq n_g$.*

In Figure 1, $X_{g,1}$ and $X_{g,2}$ are not separated operating points since both have the same velocity, but $X_{g,1}$ and $X_{g,5}$ are separated operating points.

**Assumption 2.** *There exist k operating points to satisfy the following condition for all separated operating points $X_{g,i}$ and $X_{g,j}$*

$$\max_{1\leq i\leq k}\left[\min_{1\leq j\leq k}\left\|X_{g,i} - X_{g,j}\right\|\right] < \varepsilon_2. \tag{5}$$

This assumption implies that over the operating envelope, a large number of operating points are required so that adjacent operating points are close enough. For each frozen operating point $X_{g,i}$, we can obtain a family of equilibrium states and inputs

$$\sigma_p = \left\{X_p(X_{g,1}),\ X_p(X_{g,2}),\ \cdots,\ X_p(X_{g,k})\right\} \tag{6}$$

$$\sigma_u = \left\{U_1(X_{g,1}),\ U_1(X_{g,2}),\ \cdots,\ U_1(X_{g,k})\right\} \tag{7}$$

That is,

$$f(X_p(X_{g,i}), X_{g,i}) + g(X_p(X_{g,i}), X_{g,i})U_1(X_{g,i}) = 0.$$

and $\sigma_g$, $\sigma_p$, and $\sigma_u$ are tabulated off-line. By using a linear interpolation in $\sigma_p$ and $\sigma_u$, we can construct desired trajectories of the state and the input $(X_p^*(t),\ U_1^*(t))$

$$\begin{aligned} X_p^*(t) &= X_p(X_{g,i}) + M_i(X_g(t) - X_{g,i}) \\ U_1^*(t) &= U_1(X_{g,i}) + N_i(X_g(t) - X_{g,i}) \end{aligned} \tag{8}$$

where $M_i$ and $N_i$ are constant matrices which map $X_g$ into $X_p$ and $U$ respectively. Using these trajectories, we linearize the plant in (1) about $(X_g(t),\ X_p^*(t),\ U_1^*(t))$ as

$$\dot{x}_p = A_p(t)x_p + B_p(t)u + \varepsilon_x(t) \tag{9}$$

where $x_p = X_p - X_p^*(t)$, $u = U_1 - U_1^*(t)$ and

$$A_p(t) = \left.\frac{\partial f}{\partial X_p}\right|_{(X_p^*(t), X_g(t))} + \left.\frac{\partial g}{\partial X_p}\right|_{(X_p^*(t), X_g(t))} U_1^*(t)$$

$$B_p(t) = g(X_p^*(t),\ X_g(t))$$

$$\varepsilon_x(t) = f(X_p^*(t), X_g(t)) + g(X_p^*(t), X_g(t))U_1^*(t) - \dot{X}_p^*(t) + O(x_p^2).$$

The following proposition quantifies allowable slow variations in $X_g(t)$, which is the gain-scheduling variable.

**Proposition 1.** *Under Assumptions 1 and 2,*

$$\|\varepsilon_x(t)\| \le a\varepsilon_1 + b\varepsilon_2 \tag{10}$$

*where a and b are positive constants.*

*Proof.* Due to space limitations, the proof is omitted. □

**Remark 1.** *By making $\varepsilon_1$ and $\varepsilon_2$ suitably small, $\varepsilon_x$ can be made arbitrarily small. In other words, if the gain-scheduling variable is varying sufficiently slowly, and operating points are sufficiently close to each other, $\varepsilon_x$ can be made arbitrarily small.*

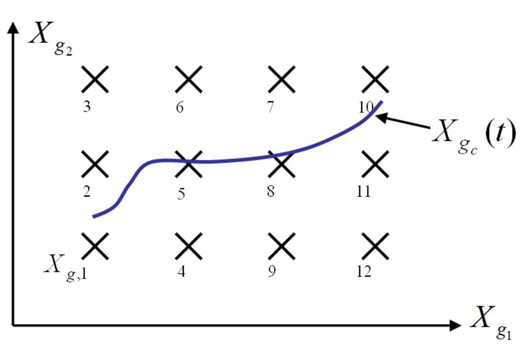


Fig. 1. A schematic of operating points the $X_g$ space($k$=12)

The problem that we consider in this paper is the control of the system in (9) subject to Assumptions 1 and 2 in the presence of uncertainties introduced due to control anomalies. In particular, we assume that the nonlinear dynamics in (2) is of the form

$$\dot{X}_p = f(X_p, X_g) + g(X_p, X_g)\Lambda U_1. \tag{11}$$

where $\Lambda$ is an unknown diagonal matrix with nonzero diagonal entries, and represents a loss of effectiveness in the control input. By linearizing the nonlinear dynamics in (11) about the same trajectory in (8), we get

$$\dot{x}_p = A_{p\lambda}(t)x_p + B_p(t)\Lambda(u + d(t)) + \varepsilon_x(t) \tag{12}$$

where

$$A_{p\lambda}(t) = \left.\frac{\partial f}{\partial X_p}\right|_{(X_p^*(t), X_g(t))} + \left.\frac{\partial g}{\partial X_p}\right|_{(X_p^*(t), X_g(t))} \Lambda U_1^*(t)$$

$$d(t) = (I - \Lambda^{-1})U_1^*(t)$$

and $d(t)$ is the input disturbance due to $\Lambda$. Therefore, when there is no uncertainty in the control input, i.e. $\Lambda = I$, $d(t)$ becomes zero. The problem is to design an adaptive augmentation of a baseline gain-scheduling controller for the plant in (12) under Assumptions 1 and 2 such that closed-loop stability and tracking is maintained in the presence of the system uncertainties.

## III. Adaptive Controller

### A. Reference Model and Baseline Controller

In order to achieve desired closed-loop dynamics in the presence of uncertainties, we propose to augment a baseline gains-scheduling controller with a direct adaptive component. For the purpose of the nominal controller design, we utilize the principles of gain-scheduling, similar to those in [1], [2], and develop a time-varying controller, under the premise that no uncertainties are present. The details of the gain-scheduled controller are given below.

We linearize the nonlinear plant in (2), where no uncertainties are present, at every frozen equilibrium point and obtain the linearized plant as

$$\dot{x}_p = A_{p,i}x_p + B_{p,i}u_i \tag{13}$$

where

$$A_{p,i} = \left.\frac{\partial f}{\partial X_p}\right|_{(X_p(X_{g,i}), X_{g,i})} + \left.\frac{\partial g}{\partial X_p}\right|_{(X_p(X_{g,i}), X_{g,i})} U_1(X_{g,i})$$

$$B_{p,i} = g(X_p(X_{g,i}),\ X_{g,i}).$$

The nominal controller at $i$th equilibrium point is chosen as

$$u_{nom,i} = K_i^\top x_p \tag{14}$$

The feedback gain matrix, $K_i$, is found by the LQR method [8] which provides suitable closed-loop responses of (13) combined with (14). The reference model at each equilibrium point is defined as

$$\dot{x}_m = A_{m,i}x_m \tag{15}$$

where $A_{m,i} = A_{p,i} + B_{p,i}K_i^\top$ and $A_{m,i}$ is Hurwitz. Since the nominal controller is designed based on several fixed equilibrium points, the controller gain needs to be interpolated or scheduled as

$$u_{nom}(t) = K(t)^\top x_p \tag{16}$$

where $K(t) = K_i + L_i(X_g(t) - X_{g,i})$ and $L_i$ is a constant matrix which represents a linear mapping from $X_g$ into $K$. Correspondingly, we choose a time-varying reference model that the plant in (12) is required to track as

$$\dot{x}_m = A_m(t)x_m \tag{17}$$

where $A_m(t) = A_p(t) + B_p(t)K(t)^\top$. It is straight forward to show that if the control input in (9) is chosen as

$$u(t) = u_{nom}(t) \tag{18}$$

under Assumptions 1 and 2, the closed-loop nonlinear system is globally bounded [14].

### B. Adaptive Controller Design

In order to maintain tracking performance in the presence of uncertainties, we augment the nominal controller with an adaptive component. The total control input $u$ in (12) is chosen as

$$u = u_{nom} + u_{ad} \tag{19}$$

The adaptive control input, $u_{ad}$, is designed as

$$u_{ad} = \theta^\top \omega \tag{20}$$

where $\theta = [\theta_x^\top \quad \theta_d^\top]^\top$, $\omega = [x_p^\top \quad 1_{1\times 3}]^\top$. It is assumed that an ideal control parameter, $\theta^*(t)$, exists such that

$$A_{p\lambda}(t)+B_p(t)\Lambda\left(K(t)+\theta_x^*(t)\right)^\top = A_m(t), \theta_d^{*\top}(t) = -d(t). \tag{21}$$

We define the tracking error to be $e = x - x_m$ and the adaptive parameter error to be $\tilde{\theta} = \theta - \theta^*$. Subtracting (17) from (12), the tracking error dynamics is obtained as

$$\dot{e} = A_m(t)e + B_p(t)\Lambda\tilde{\theta}^\top\omega + \varepsilon_x(t). \tag{22}$$

The adaptive law is designed as in [9]

$$\dot{\theta} = -\Gamma\omega e^\top PB_p(t)sign(\Lambda) - \theta\left(1 - \frac{\|\theta\|}{\theta^*_{\max}}\right)^2 f(\theta) \tag{23}$$

where

$$f(\theta) = \begin{cases} 1 & \text{if } \|\theta\| > \theta^*_{\max} \\ 0 & \text{otherwise.} \end{cases}$$

$P = P^\top > 0$ is the solution of $A_m^\top P + PA_m = -Q$ for a given $Q = Q^\top > 0$, $\Gamma > 0$ is a diagonal matrix which represents adaptation rate, $sign(\Lambda) = diag\left(sign(\lambda_1), \cdots, sign(\lambda_{m_1})\right)$, $\|\theta^*\| \leq \theta^*_{\max}$, $\theta^*_{\max}$ is a known constant.

## IV. STABILITY ANALYSIS

Since the adaptive control basically attempts to enforce the unknown plant to track a given reference model, stability of the reference model should be guaranteed first.

**Assumption 3.** *Given $Q = Q^\top > 0$, there exist $P(t) = P^\top(t) > 0$ and $\varepsilon_3 > 0$ such that*

$$A_m^\top(t)P(t) + P(t)A_m(t) = -Q, \quad \left\|\dot{P}\right\| \leq \varepsilon_3 < q_0 \tag{24}$$

*where $q_0 = \min eig(Q)$.*

The above assumption implies that $P(t)$, and $A_m(t)$, are slowly varying. This, in turn, implies that time-derivative of the positive definite function

$$W = x_m^\top P(t)x_m \tag{25}$$

along (17) is given by

$$\dot{W} = x_m^\top(-Q + \dot{P})x_m \leq -x_m^\top(q_0 - \varepsilon_3)x_m < 0. \tag{26}$$

and hence the origin is the asymptotically stable equilibrium of (17).

**Remark 2.** *Assumption 3 is introduced primarily for the purpose of accommodating a linear time-varying reference model as in* (17). *Such a reference model may often be desired in an application in order to accommodate different transient characteristics at different points in the operating envelope.*

We now prove the main result of the paper.

**Theorem 1.** *Under Assumptions 1, 2, and 3, the plant in* (12) *with the controller in* (19) *and the adaptive law in* (23)*, has globally bounded solutions for all $t \geq t_0$.*

*Proof.* A Lyapunov candidate function is chosen as

$$V = e^\top Pe + trace\left(\tilde{\theta}^\top\Gamma^{-1}\tilde{\theta}|\Lambda|\right) \tag{27}$$

where a time-derivative is given by

$$\begin{aligned}\dot{V} = &-e^\top\left(Q - \dot{P}\right)e + 2e^\top P\varepsilon_x - 2trace\left(\tilde{\theta}^\top\Gamma^{-1}\dot{\theta}^*\right) \\ &- 2trace\left[\tilde{\theta}^\top\Gamma^{-1}\theta|\Lambda|\left(1 - \frac{\|\theta\|}{\theta^*_{max}}\right)^2 f(\theta)\right]\end{aligned} \tag{28}$$

where $|\Lambda| = sign(\Lambda)\Lambda$.

Two cases are considered, $(i)\ \|\theta\| \leq \theta^*_{\max}$ and $(ii)\ \|\theta\| \geq \theta^*_{\max}$.

*Case (i)*: $\|\theta\| \leq \theta^*_{\max}$

$\|\theta\| \leq \theta^*_{\max}$ implies that $\|\tilde{\theta}\| \leq 2\theta^*_{\max}$ and $f(\theta) = 0$ from which we obtain

$$\dot{V} = -e^\top\left(Q - \dot{P}\right)e + 2e^\top P\varepsilon_x - 2trace\left(\tilde{\theta}^\top\Gamma^{-1}\dot{\theta}^*\right). \tag{29}$$

By taking bounds on the right-hand side of (29), we have

$$\dot{V} \leq -\left(q_o - \varepsilon_1\right)\|e\|^2 + 2\|P\|\|\varepsilon_x\|\|e\| + 2\frac{\|\dot{\theta}^*\|}{\gamma_{\min}}\|\tilde{\theta}\| \tag{30}$$

where $\gamma_{\max(\min)}$ is the maximum(minimum) of the diagonal elements of $\Gamma$. Hence, $\dot{V} \leq 0$ outside of the compact set

$$D_1 = \left\{\left(e, \tilde{\theta}\right)\middle|\left(\|e\| - \frac{\|P\|\|\varepsilon_x\|}{q_o - \varepsilon_1}\right)^2 \leq k_1, \|\tilde{\theta}\| \leq 2\theta^*_{\max}\right\} \tag{31}$$

where

$$k_1 = \frac{4\|\dot{\theta}^*\|\theta^*_{\max}}{\gamma_{\min}(q_o - \varepsilon_1)} + \frac{\|P\|^2\|\varepsilon_x\|^2}{(q_o - \varepsilon_1)^2}.$$

This implies $(x(t),\ \theta(t))$ are globally bounded.
*Case (ii)*: $\|\theta\| \geq \theta^*_{\max}$
Time derivative of $V$ in (27) becomes

$$\begin{aligned}\dot{V} =& -e^\top\left(Q-\dot{P}\right)e+2e^\top P\varepsilon_x - 2trace\left(\tilde{\theta}^\top\Gamma^{-1}\dot{\theta}^*\right)\\ & -2trace\left(\tilde{\theta}^\top\Gamma^{-1}\theta|\Lambda|\right)\left(1-\frac{\|\theta\|}{\theta^*_{\max}}\right)^2\end{aligned} \tag{32}$$

From (32), we have the following inequality as

$$\begin{aligned}\dot{V} \leq& -(q_o-\varepsilon_3)\|e\|^2+2\|P\|\|\varepsilon_x\|\|e\|+2\frac{\|\dot{\theta}^*\|}{\gamma_{\min}}\|\tilde{\theta}\|\\ & -2\frac{\lambda_{\min}}{\gamma_{\max}}\|\tilde{\theta}\|\left(\|\tilde{\theta}\|-\frac{\lambda_{\max}\gamma_{\max}}{\lambda_{\min}\gamma_{\min}}\|\theta^*\|\right)\left(1-\frac{\|\theta\|}{\theta^*_{\max}}\right)^2\end{aligned} \tag{33}$$

where $\lambda_{\max(\min)}$ is the maximum(minimum) of the diagonal elements of $|\Lambda|$. We define a constant $a_0$ and $K$ by

$$a_0 = \frac{\lambda_{\max}\gamma_{\max}}{\lambda_{\min}\gamma_{\min}},\ K = 1+a_0+\varepsilon_4 \quad \varepsilon_4>0. \tag{34}$$

We consider two sub-cases as follows.
*Sub-case (a)*: $\theta^*_{\max} < \|\theta\| \leq K\theta^*_{\max}$
For a given condition on $\|\theta\|$, we have the following inequalities while using $K-1 = a_0+\varepsilon_4$

$$\begin{aligned}&\|\tilde{\theta}\| \leq (K+1)\theta^*_{\max},\ \left(1-\frac{\|\theta\|}{\theta^*_{max}}\right)^2 \leq (a_0+\varepsilon_4)^2\\ &\|\tilde{\theta}\|-\frac{\lambda_{\max}\gamma_{\max}}{\lambda_{\min}\gamma_{\min}}\|\theta^*\| \leq (K+1+a_0)\theta^*_{\max}.\end{aligned} \tag{35}$$

Consequently,

$$\begin{aligned}\dot{V} \leq& -(q_o-\varepsilon_3)\|e\|^2+2\|P\|\|\varepsilon_x\|\|e\|+2\frac{\|\dot{\theta}^*\|}{\gamma_{\min}}\|\tilde{\theta}\|\\ & +2\frac{\lambda_{\min}}{\gamma_{\max}}(K+1)(K+1+a_0)(a_0+\varepsilon_4)^2\theta^{*2}_{\max}\end{aligned} \tag{36}$$

Therefore, $\dot{V} \leq 0$ outside of the compact set

$$D_2 = \left\{(e,\tilde{\theta})\middle|\left(\|e\|-\frac{\|P\|\|\varepsilon_x\|}{q_o-\varepsilon_3}\right)^2 \leq k_2, \|\tilde{\theta}\| \leq (K+1)\theta^*_{\max}\right\} \tag{37}$$

where

$$\begin{aligned}k_2 =& \frac{2(K+1)\|\dot{\theta}^*\|\theta^*_{\max}}{\gamma_{\min}(q_o-\varepsilon_3)}+\frac{\|P\|^2\|\varepsilon_x\|^2}{(q_o-\varepsilon_3)^2}\\ & +\frac{2\lambda_{\min}(K+1)(K+1+a_0)(a_0+\varepsilon_4)^2\theta^{*2}_{\max}}{\gamma_{\max}(q_o-\varepsilon_3)}.\end{aligned}$$

Since $k_2 > k_1$, we note that $D_2 \supset D_1$.
*Sub-case (b)*: $\|\theta\| > K\theta^*_{\max}$
In this case, we get:

$$\begin{aligned}&\|\tilde{\theta}\| \geq (a_0+\varepsilon_4)\theta^*_{\max},\ \left(1-\frac{\|\theta\|}{\theta^*_{\max}}\right)^2 \geq (a_0+\varepsilon_4)^2,\\ &\|\tilde{\theta}\|-\frac{\lambda_{\max}\gamma_{\max}}{\lambda_{\min}\gamma_{\min}}\|\theta^*\| \geq \|\tilde{\theta}\|-a_0\theta^*_{\max} \geq \frac{\varepsilon_4}{a_0+\varepsilon_4}\|\tilde{\theta}\|.\end{aligned} \tag{38}$$

Using (33), we obtain:

$$\begin{aligned}\dot{V} \leq& -(q_o-\varepsilon_3)\|e\|^2+2\|P\|\|\varepsilon_x\|\|e\|\\ & -2\frac{\lambda_{\min}}{\gamma_{\max}}\varepsilon_4(a_0+\varepsilon_4)\|\tilde{\theta}\|^2+2\frac{\|\dot{\theta}^*\|}{\gamma_{\min}}\|\tilde{\theta}\|.\end{aligned} \tag{39}$$

Hence, outside of the compact set

$$\begin{aligned}D_3 = \Bigg\{(e,\tilde{\theta})\,\Bigg|\,&\left(\|e\|-\frac{\|P\|\|\varepsilon_x\|}{q_o-\varepsilon_3}\right)^2\\ &+\frac{k_3}{q_o-\varepsilon_3}\left(\|\tilde{\theta}\|-\frac{\|\dot{\theta}^*\|}{\gamma_{\min}k_3}\right)^2 \leq k_4\Bigg\}\end{aligned} \tag{40}$$

with

$$k_3 = 2\frac{\lambda_{\min}}{\gamma_{\max}}\varepsilon_4(a_0+\varepsilon_4),\ k_4 = \frac{\|P\|^2\|\varepsilon_x\|^2}{(q_o-\varepsilon_3)^2}+\frac{\|\dot{\theta}^*\|^2}{\gamma^2_{\min}k_3(q_o-\varepsilon_3)}$$

all signals are bounded. We define a compact set $D$ to be $D = D_2 \cup D_3$. Then, outside of $D$, $\dot{V} \leq 0$ and this guarantees global boundedness of $(e,\ \tilde{\theta})$, which implies of boundedness of $x_p$ and $\theta$. This, in turn, proves that the control input $u$ is globally bounded. □

**Remark 3.** *The above proof establishes that outside the compact set, $\dot{V} < 0$, which in turn implies that all trajectories converge to the compact set. This in turn implies that the tracking error is of the order of the variations in the gain-scheduling variable.*

## V. SIMULATIONS

In this section, we demonstrate efficiency of the proposed controller using a nonlinear 6-DOF high performance aircraft simulation environment [10]. Aerodynamic model of the NASA X-15 discussed in [11] is employed to validate the proposed adaptive controller. Dynamics of the NASA X-15 aircraft can be cast into the form of (2)

$$\begin{aligned}&X_p = [\alpha \quad \beta \quad p \quad q \quad r]^\top, \quad U_1 = [\delta_a \quad \delta_{e_2} \quad \delta_r]^\top\\ &X_g = [V \quad h]^\top, \quad U_2 = [\delta_{e_1} \quad \delta_T]^\top.\end{aligned}$$

Right and left elevons are employed as pitch (elevator) and roll (aileron) devices by

$$\delta_e = \frac{1}{2}\left(\delta_{Left}+\delta_{Right}\right),\ \delta_a = \frac{1}{2}\left(\delta_{Left}-\delta_{Right}\right). \tag{41}$$

### A. Nominal Controller Design

The nominal controller consists of two controllers: outer-loop and inner-inner loop. The outer-loop controller is used to adjust $V$ and $h$, and two fixed PID (with approximated derivative) controllers to ensure that $V$ and $h$ track the desired commanded signals $V_{cmd}$ and $h_{cmd}$, respectively. These are designed using errors between the actual and commanded signals. The PID gains are tuned based on Ziegler-Nichols tunning rule [12]. 44 operating points are selected for nominal (inner-loop) controller design as shown in Figure 2 in $(V,\ h)$ space. Intervals between the operating points are selected such that linearization error, $\varepsilon_x(t)$, in (12) is sufficiently small. During the first 160 seconds, the

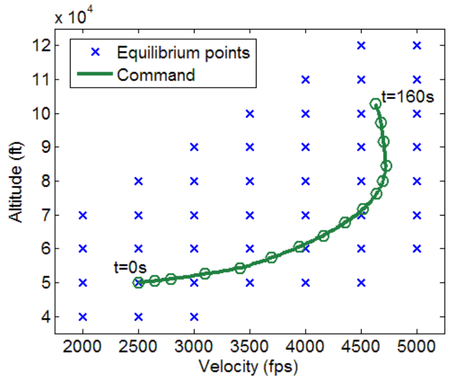


Fig. 2. Operating points on $V$-$h$ diagram and command $X_{g_c}$.

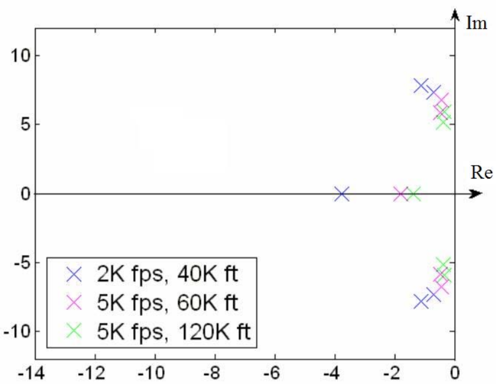


(a) Open-loop plants, $A_{p,i}$

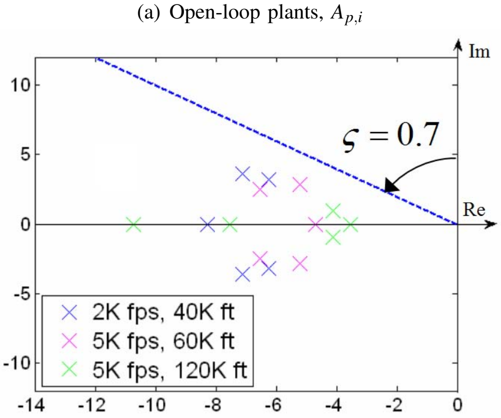


(b) Reference models, $A_{m,i}$

Fig. 3. Poles of the open-loop plants and the reference models

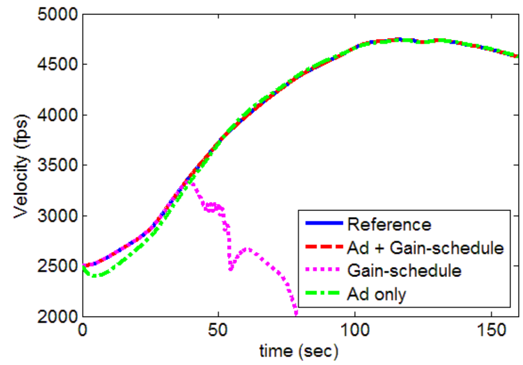


(a) Velocity

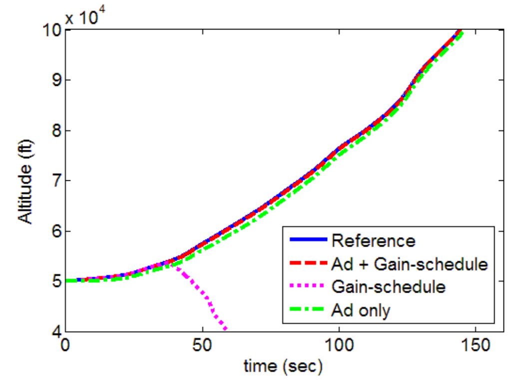


(b) Altitude

Fig. 4. Velocity and altitude profile in the presence of control failure

command, $X_{g_c}$, is given as shown in Figure 2. The initial altitude is $50,000$ft and it increases up to $100,000$ft, while the velocity increases by more than $4,500$fps (Mach 5). Green circles on the command line in Figure 2 represent way-points for every 10s. By linearizing the nonlinear plant in (2), we obtain $A_{p,i}$ and $B_{p,i}$, and design the inner loop nominal controller for each operating points. Figure 3(a) shows pole location of the open-loop system at three different operating points: (2,000fps, 40,000ft), (5,000fps, 60,000ft), and (5,000fps, 120,000ft). One can see that characteristics of the plant change significantly depending on the operating points. This observation justifies the use of a gain-scheduling controller. In Figure 3(b), poles of the reference model are shown for the same three operating points. As seen in Figure 3(b), poles of the reference models at different operating points are located close to each other, which ensures that $A_m(t)$ is slowly varying. This, in turn, implies that $P(t)$ is slowly varying. Thus, Assumption 3 holds.

### *B. Simulation Results*

The control failure $\Lambda = diag([1\ 0.8\ 1])$ is introduce at 30s. This failure implies 20% loss of the right flap effectiveness. The adaptive controller is placed in the outer loop of the nominal controller where the adaptation rate $\Gamma$ is chosen based on the heuristic method from [13]. In practice, the NASA X-15 aircraft model has input saturation limits. We included these input constraints in the simulation studies. Actuator limits for the elevator, aileron,and rudder surfaces were set to: $\pm 30$, $\pm 30$, and $\pm 15$ degrees, correspondingly.

Figure 4shows simulation results, that were obtained using the proposed controller. It can be seen that the adaptive controller ensures satisfactory command following while the nominal controller fails to stabilize the plant. Figure 5 shows the closed-loop system state variables which include angle of attack ($\alpha$), sideslip angle ($\beta$), roll rate ($p$), pitch rate ($q$), and yaw rate ($r$). When the control failure occurs at 30s, the system becomes unstable with the nominal controller whereas with the added adaptive controller, the instability is removed and the desired tracking performance is restored. For comparison purposes, the case where only

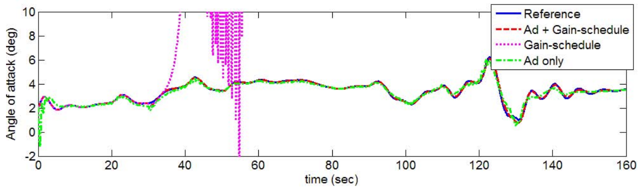


(a) $\alpha$

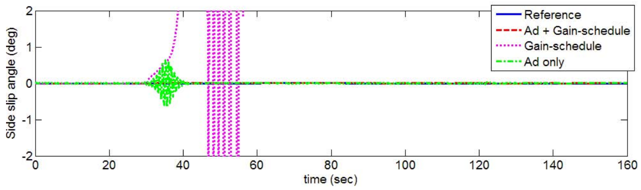


(b) $\beta$

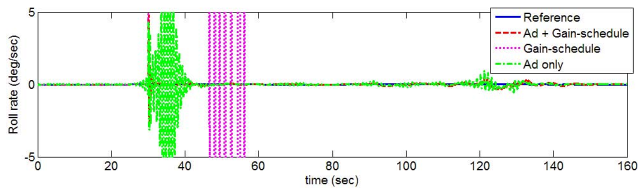


(c) $p$

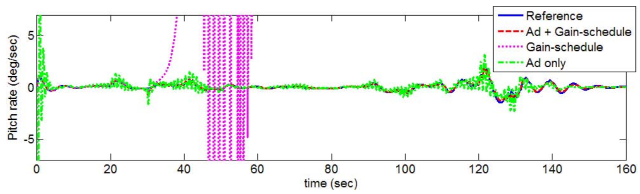


(d) $q$

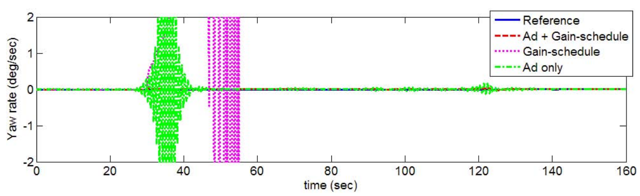


(e) $r$

Fig. 5. State variables

the adaptive controller is used without the baseline gain-scheduling controller is also simulated. Even though stability is guaranteed in this case, it has undesirable oscillations when the control failure occurs. This demonstrates that the augmented adaptive controller inherits a better performance. Control inputs are shown in Figure 6. With only the nominal controller, the control inputs grow unbounded.

## VI. CONCLUSIONS

In this paper, we proposed a systematic control design procedure for a class of nonlinear uncertain dynamic systems. Our control architecture consisted of a nominal baseline-controller and a direct adaptive model-following controller. The adaptive law was derived based on the Lyapunov stability theory. We presented sufficient conditions for uniform boundedness of the closed-loop dynamics. Nonlinear 6-DOF flight dynamics of a hypersonic aircraft is employed to validate stability, performance, and robustness of the proposed robust adaptive flight controller.

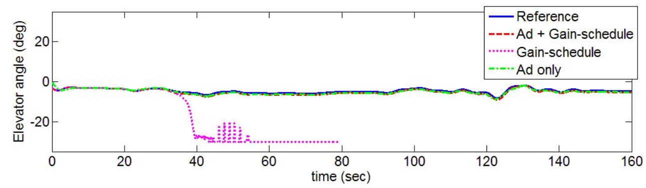


(a) Elevator

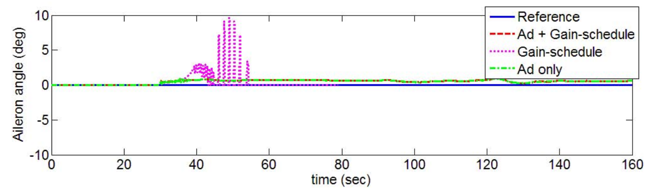


(b) Aileron

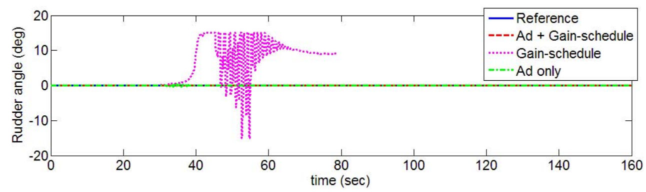


(c) Rudder

Fig. 6. Control surfaces

## REFERENCES

[1] W. J. Rugh and J. S. Shamma, "Research on gain scheduling," *Automatica*, vol. 36, pp. 1401-1425, 2000.

[2] D. J. Leith and W. E. Leithead, "Survey of gain-scheduling analysis and design," *International Journal of Control*, vol. 73, no. 11, 1001-1025.

[3] L. H. Lee and M. Spillman, "Control of slowly varying LPV systems: an application to flight control," *Proceedings of the Conference on Decision and Control*, San Diego, CA, 1997.

[4] R. A. Nichols, R. T. Reichert, and W. J. Rugh, "Gain scheduling for $H_\infty$ controllers: a flight control example," *IEEE Transactions on Control System Technology*, vol. 1, no. 2, pp. 69-78, 1993.

[5] S. J. Qin and G. Borders, "Multi-region fuzzy logic control system with auxiliary variables," *IEEE Transactions on Fuzzy Systems*, vol. 2, no. 1, pp. 74-89, 1994.

[6] D. J. Leith and W. E. Leithead, "Appropriate realisation of gain scheduled controllers with application to wind turbine regulation," *International Journal of Control*, vol. 65, pp. 223-248, 1996.

[7] J. Reeve and M. Sultan, "Gain scheduling adaptive control strategies for HVDC systems to accommodate large disturbances," *IEEE Transactions on Power Systems*, vol. 9, no. 1, pp. 366-372, 1994.

[8] G. F. Franklin, J. D. Powell, and A. Emami-Naeini, *Feedback control of dynamic systems*, Upper Saddle River, NJ: Prentice Hall, 2006.

[9] G. Kreisselmeier and K. S. Narendra, "Stable model reference adaptive control in the presence of bounded disturbances," *IEEE Transactions on Automatic Control*, vol. 27, no. 6, pp. 1169-1175, Dec. 1982.

[10] D. G. Ward et al., "Intelligent Control of Unmanned Air Vehicles Program Summary and Representative Results," *Proceedings of 2nd AIAA "Unmanned Unlimited" Systems, Technologies, and Operations-Aerospace, Land, and Sea Conference and Workshop & Exhibit*, 2003.

[11] E. C. Holleman, "Summary of High-Altitude and Entry Flight Control Experience with the X-15 Airplane," NASA TN D-3386, April 1966.

[12] J. G. Ziegler and N. B. Nichols, "Optimum Settings for Automatic Controllers," *Trans. ASME*, vol. 64, pp. 759-768, 1942.

[13] Z. Dydek et al., "Theoretically Verifiable Stability Margins for an Adaptive Controller," *Proceedings of AIAA Guidance, Navigation, and Control Conference and Exhibit*, Keystone, Colorado, Aug. 2006.

[14] J. S. Shamma, "Analysis and design of gain scheduled control systems," Ph.D. Dissertation, Department of Mechanical Engineering, MIT, Cambridge, 1988.